# Constitutive modeling for rock joints of tunnel

## 터널 암반절리에 대한 구성방정식 모델링

박인준*
Park, Inn-Joon

**Abstract**

The purpose of this research is to develop improved model for joints of tunnel based on Disturbed State Concept (DSC) model. DSC model is verified with respect to comprehensive laboratory tests performed by Schneider and back prediction results. Based on results of this research, it can be stated that DSC model is capable of characterizing the strain softening and dilative behavior of rough granite joints under four different constant normal stresses.

**Keywords:** Joints, disturbed state concept, back prediction, softening, dilative behavior

**요 지**

본 연구의 목적은 교란상태개념 (DSC) 모델을 이용하여 터널 암반절리면의 거동특성을 모델링 할 수 있는 개선된 구성방정식 모델을 개발하는데 있다. 교란상태 개념 (DSC) 모델은 이미 다른 접촉면 거동 모델링을 통해서 그 신뢰성을 검증 받아왔다. 이런 DSC 모델을 암반 절리면 거동 특성에 맞도록 수정한 후에, Schneider가 수행한 합리적인 실내 전단 시험 결과 및 역 해석 결과를 이용하여 DSC모델의 절리면 적용성을 검증하고자 한다. 본 연구결과로부터 DSC모델은 화강암 절리면의 변형률 연화 및 부피팽창 거동특성을 규명할 수 있다고 판단된다.

**주요어:** 암반 절리, 교란상태개념, 역 해석, 변형률 연화, 부피팽창 거동

## 1. Introduction

In practice, we meet a number of problems associated with rock joints and discontinuities. In tunnel engineering, stability of supporting columns which contain rock joints or faults is a main concern. And in geotechnical engineering, they have problems such as slope stability, foundation and underground openings, which are related to the behavior of rock joints and faults involved. Therefore, joints, faults, and discontinuities play a vital role in rock and tunnel engineering practices.

The behavior of the discontinuous joints is different from that of the continuous solid materials. The shear strength of a solid comes from the strong internal cohesion, while the shear strength of a joint

*Member, Hanseo University, Professor.

is mainly derived from contact friction which involves many types of mechanisms, such as interlocking, ploughing, and damaging of the asperities. Therefore, the modeling of the joints involves significant complexity and is very important. Rational constitutive models can only be obtained through careful study of their special features in addition to those of continuous solids, and also through consideration of the basic mechanics and laboratory testing and verification.

This research aims to investigate the strength and deformation behavior of the joints or discontinuities under various loading conditions. The objectives of the investigation can be summarized as follows:

1) To modify the disturbed state concept theory for its application to the rock joint modeling.
2) To develop the model capable of describing and predicting the hardening and softening behavior of the rock joints under various stress path conditions.
3) To utilize the proposed model and verify it with respect to experimental data on rock joints.
4) To analyze the size effect of the joints in modelling.

Several models have been developed for defining the behavior of joint. There are two types of joint models: failure model and elasto-plastic model.

## 1.1 Failure models

Failure models describe the shear stress in relation to the normal stress and other parameters. This relation is generally nonlinear as long as the range of the normal stress is wide enough. Usually, the shear stress reaches a peak value and then decreases to a residual value. This phenomenon is termed softening as found in most rocks (Goodman, 1974; Hoek and Bray, 1974). In failure models, emphasis is focused mainly on the modeling of peak and residual shear stresses.

Barton and Chouby(1977) proposed a failure model for peak shear strength of rock joints after summarizing extensive tests upon specially prepared artificial rock joints. The peak shear strength was expressed as

$$\tau_p = \sigma_n \tan\left[JRC\log\left(\frac{JCS}{\sigma_n}\right) + \Phi_b\right] \quad (1)$$

where JRC and JCS are the Joint Roughness Coefficient and Joint Compression Strength respectively, and $\Phi_b$ is the residual friction angle. Schneider(1975) modified Patton's bilinear model by combining the angle of asperities of natural rock joints.

Most failure models described the above attempt to relate the shear strength of a rough joint with the slope angle or the shear strength with the strength of the asperities. However, failure models do not give the description of the stress-strain relationship which is necessary for calculations involved with displacements other than the strength of the joints. The elastic and elasto-plastic models are capable of providing the stress-strain relationship as discussed below.

## 1.2 Elastic and elasto-plastic models

Goodman, Taylor, and Brekke (1971) proposed a nonlinear model for rock joints. This model has the off-diagonal terms of the stiffness matrix which are considered as the coupling terms between the shear and normal behavior. Ghaboussi and Wilson (1973) proposed the possible application of the plasticity theory in joint modeling by assuming the association flow rule. The yield functions used here are the Mohr-Coulomb failure law for non-dilatant joint, and the Cap (DiMaggio and Sandler, 1971) model of yield functions for dilatant joint. Zienkiwicz *et al.* (1977)

proposed an elastic-viscoplastic model for joint. The yield function F used is the Mohr-Coulomb failure law. Both associative and non-associative potential function Q has a similar type as the yield function. Plesha (1987) proposed a non-associative plasticity joint model. The main feature of this model is to use a parameter called the asperity angle to characterize the strength and deformation behavior of the joint. At the same time, Desai and Fishman (1987) developed a non-associative plasticity model by specializing a general 3-D Hierarchical Single Surface model (HiSS Model) (Desai *et al.*, 1984, 1986). The yield function F and the displacement potential function Q are expressed as

$$F = \tau^2 + \alpha\sigma_n^n - \gamma\sigma_n^2 = 0 \quad (2)$$

$$Q = \tau^2 + \alpha_Q\sigma_n^n - \gamma\sigma_n^2 = 0 \quad (3)$$

where n and $\gamma$ are material constants, $\alpha$ is the hardening function, and $\alpha_Q$ is the non-associative hardening function. This model can be used for both quasi-static and cyclic loading conditions. However, softening can not be captured.

In this paper, a modified version of Disturbed State Concept (DSC) model (Desai, 1992; Desai, 1995; Park, 1997) is proposed to model both hardening and softening behavior with a frame-work that can include a number of important characteristics of joints

## 2. Disturbed sate concept modeling for joint of rock

The disturbed state concept (DSC) extends cont-inuum theory representations of material behavior to include observed nonhomogeneous and discont-inuous behavior such as microcracking, damage, and softening. It is based on the DSC that allows incorporation of microstructural changes due to the applied forces, that cause transitions in the material from relative intact (RI) state, through a process of natural self adjustment, to the fully adjusted or critical (FA) state. The process of transition from the RI to FA state involves changes in the microst-ructural properties of the joint material, affected by factors such as roughness, asperities, particle size and shape, and interparticle characteristics. The observed material behavior is thus defined as a combination of the two material reference states, RI state and FA state, which are related through the disturbance function, D (Fig. 1). The concept of the disturbed state of a joint can be expressed by the two reference states (RI and FA) and D.

The disturbed state for a joint is the inter-mediate state from the original state until the critical state is researched. During the disturbed state, the damageable material and non-damageable material co-exist. From the DSC theory for a joint material (Desai, 1995), the damageable material repres-ents those asperities that are broken or lose contact during shearing, and those contacts that are separated by the debris. The non-damageable material repres-ents those asperities that are not breakable for the given normal stress, and would include plateaus formed and compacted gouge material formed during shearing. Consequently, strain softening may result if the joint becomes smoother.

To best describe the various references states for jointed rock, a simple example is presented herein. Consider a bucket filled with ice. When heated, the ice will thaw into water. The ice represents the material in its original state or RI state, while the water represents the material in FA state, and heating is the factor that causes the disturbance, D. During the period starting from ice (RI state) and ending with water (FA state), there are many inter-mediate states where the container includes both ice

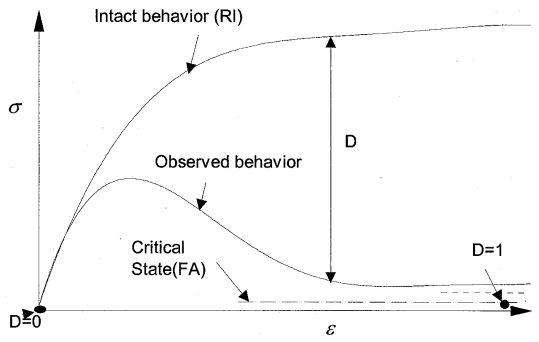


Fig. 1 Schematic of stress-strain behavior (after Park, 1997).

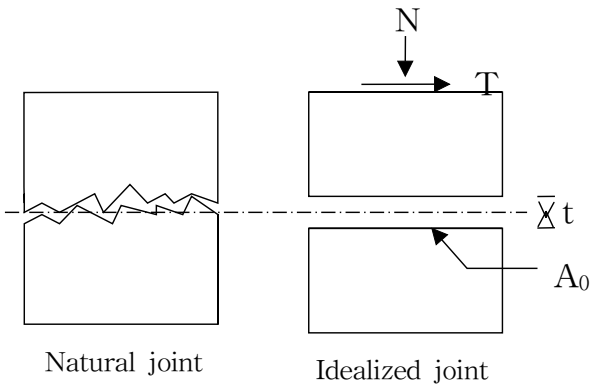


Fig. 2 Idealization of a joint.

and water. These intermediate states are said to be in the disturbed state. During the disturbed state, the ice changes gradually to water and there exists a mixture of ice and water.

## 2.1 Idealization of a joint

A joint is the region of two opposing surfaces of two contacting solids. The physical properties of a joint are determined by these two surfaces and their contact conditions. To mathematically model a joint or interface, the joint is usually considered as a planar surface with two joint walls and a contact space (Fig. 2). Here, the contact space is the contact zone of the opposing asperities and it can be assigned as averaged thickness t. A coordinate system can be established where the planar surface is considered; the tangential direction with shear stresses $\tau$, and relative shear displacements $u^r$, and the direction orthogonal to the planar surface is the normal direction with normal stresses $\sigma_n$, and relative normal displacement $v^r$. If T and N are the tangential and normal forces applied (Fig. 2), and $A_0$ is the nominal joint area, then the normal and shear stresses are:

$$\tau = \frac{T}{A_0} \tag{4}$$

$$\sigma = \frac{N}{A_0} \tag{5}$$

The relative shear displacement $u^r$, in contact zone is composed of elastic shear deformation of the contact asperities $u^e$, plastic shear deformation of the contact asperities $u^p$, and slip displacement between the contact asperities of the joint, $u^s$

$$u^r = u^e + u^p + u^s \tag{6}$$

In an analogous manner, the relative normal displacement, $v^r$, can be defined as

$$v^r = v^e + v^p + v^s \tag{7}$$

If small strains are assumed, the joint thickness, t, can be used to convert relative displacements into equivalent strains. As $t$ comes to zero, the in-plane strain $\varepsilon_x$ converges to zero and can be negligible. In view of this, the in-plane stress, $\sigma_x$, will also be small and can be negligible, particularly when the Poisson's ratio, $\nu$, is small. In terms of two-dimensional idealization, the strain-displacement

relations are

$$\begin{pmatrix} \varepsilon_x \\ \varepsilon_n \\ \gamma \end{pmatrix} = \begin{pmatrix} 0 \\ v_r/t \\ u_r/t \end{pmatrix} \tag{8}$$

and the related stress components are

$$\begin{pmatrix} \sigma_x \\ \sigma_n \\ \tau \end{pmatrix} = \begin{pmatrix} 0 \\ N/A_0 \\ T/A_0 \end{pmatrix} \tag{9}$$

## 2.2 Description of the RI state

The relative intact state is described using the modified HiSS $\delta_0$ model (Desai and Wathugala, 1987). The $\delta_0$ model is based on the associative plasticity and isotropic hardening (potential function Q = yield function F) rule. In this model, the yield function, F, is given as:

$$F = \tau^2 + \alpha \sigma_n^n - \gamma \sigma_n^2 \tag{10}$$

where $\tau$ is the shear stress, $\sigma_n$ is the normal stress, and n and $\gamma$ are material parameters. $\alpha$ is the hardening function and it is expressed as

$$\alpha = \frac{a}{\xi_D^b} \tag{11}$$

where a and b are material parameters and trajectory of plastic shear strain, $\xi_D$, is given as:

$$\xi_D = \int |d\gamma^p| \tag{12}$$

The yield surface F is a continuous set of convex surface which expands toward an ultimate yield surface during plastic shear deformation. The ultimate surface, $\tau_{ult}$, which represents the asymptotic failure stress, is found by setting $\alpha$ equal to zero:

$$\tau_{ult} = \sqrt{\gamma}\,\sigma_n \tag{13}$$

This plots a straight line with slope $\sqrt{\gamma}$ as shown in Fig. 3. The locus of points expanding yield surface (where the tangent to the yield surface is parallel to the $\sigma_n$ axis) is a line called the "Phase Change Line". By taking F=0 and $\frac{\partial F}{\partial \sigma_n} = 0$, Eq. (12) reduced to

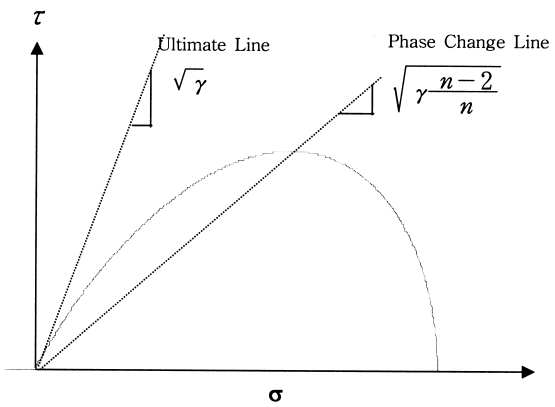


Fig. 3 The yield surface of HiSS $\delta_0$ model in $\sqrt{J_{2D}} - J_1$ space.

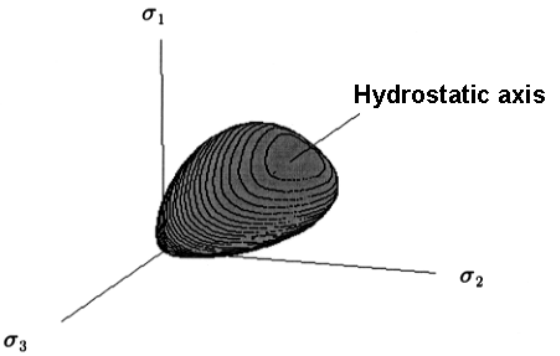


Fig. 4 The yield surface of HiSS $\delta_0$ model in stress space.

$$\frac{\tau}{\sigma_n} = \sqrt{\chi\left(\frac{n-2}{n}\right)} \tag{14}$$

The phase change line also plots as a straight line with slope $\sqrt{\chi\frac{n-2}{n}}$ in $\tau$ vs. $\sigma_n$ space (Fig. 3) and in stress space (Fig. 4).

## 2.3 Description of the FA state

The critical state is a steady state where the shear stresses and normal displacement are stabilized. The joint model at the critical state consists of two parts: the modeling of the critical shear stress and the modeling of the critical dilation. The failure model proposed by Archard (1958) is a simple one yet it gives a very good description of the shear stress at the critical state. Archard's non-linear power law model can be expressed as follows:

$$\tau^c = C_0 \sigma_n^m \tag{15}$$

where $C_0$ and m are material parameters and the superscript c refers to the critical condition. And the final dilation at the critical state, $v^c$, is found to have a relation with the normal stress (Schneider, 1975), as

$$v^c = v^0 \exp(-k\sigma_n) \tag{16}$$

where $v^0$ is the maximum dilation when $\sigma_n$ is equal to zero and k is a material parameter.

## 2.4 Description of DSC function

The proposed function for D (scalar) employed in this research was used by Armaleh and Desai (1990):

$$D = D_u[1 - \exp(-A\xi_D^Z)] \tag{17}$$

where $D_u$ is the ultimate disturbance. Initially with no disturbance the material is assumed to be entirely in the RI state, so D is zero. With full disturbance the material is assumed to be fully in FA state, and at an ultimate state, $D_u$. Theoretically, the disturbance, D, varies between 0 and 1, but many materials fail in an engineering sense before D reaches unity. A and Z are material parameters. This disturbance function will be used twice to define a shear stress relationship using disturbance, $D_\tau$, and an effective normal stress relationship using disturbance, $D_n$. Each curve in Fig. 5 is a representation of Eq. (20).

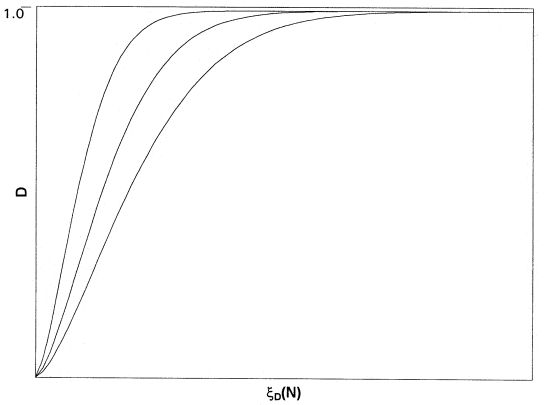


Fig. 5 Schematic of DSC function (after Park, 1997).

# 3. Incremental formulation for back prediction program

## 3.1 Derivation of the intact incremental stress-strain relation

Derivation of the intact incremental stress-strain relations follows the traditional elastoplasticity formulation procedure (Desai and Wathugala, 1987). Let the following vectors be defined

$$\{d\sigma\} = \begin{Bmatrix} d\sigma_n \\ d\tau \end{Bmatrix} \tag{18}$$

$$\{d\varepsilon\} = \begin{Bmatrix} d\varepsilon_n \\ d\gamma \end{Bmatrix} \tag{19}$$

From the elastic stress-strain relationship and the flow rule for plasticity, an incremental form of the intact stress vector can be found as

$$\{d\sigma^i\} = [C^e](\{d\varepsilon\} - \lambda\{n^F\}) \tag{20}$$

where $[C^e]$ is the elastic constitutive matrix and is given by,

$$[C^e] = \begin{bmatrix} tk_n & 0 \\ 0 & tk_s \end{bmatrix} \tag{21}$$

where $k_n$ and $k_s$ are the normal and shear stiffness of the interface material. And employing the consistency condition of the yield function (dF=0), $\lambda$ can be found as

$$\lambda = \frac{\left\{\frac{\partial F}{\partial \sigma^i}\right\}^T [C^e]\{d\varepsilon\}}{\left\{\frac{\partial F}{\partial \sigma^i}\right\}^T [C^e]\{n^F\} - \frac{\partial F}{\partial \alpha}} \tag{22}$$

and substituted into Eq. (20) to yield the constitutive relationship desired,

$$\{d\sigma^i\} = [C^{ep}]\{d\varepsilon\} \tag{23}$$

where the elasto-plastic matrix takes the form

$$[C^{ep}] = \left[ [C^e] - \frac{[C^e]\left\{\frac{\partial F}{\partial \sigma^i}\right\}\{n^F\}^T[C^e]}{\left\{\frac{\partial F}{\partial \sigma^i}\right\}^T [C^e]\{n^F\} - \frac{\partial F}{\partial \alpha} L} \right] = \begin{bmatrix} C_{nn}^{ep} & C_{ns}^{ep} \\ C_{sn}^{ep} & C_{ss}^{ep} \end{bmatrix} \tag{24}$$

where L is defined as

$$L = \frac{\partial \alpha}{\partial \xi_D} \langle n_s^F \rangle = -ab\xi_D^{b-1} \langle n_s^F \rangle \tag{25}$$

for the hardening function defined in Eq. (25) where $\langle\ \rangle$ are McAuley's brackets.

$$\begin{cases} \langle n_i^F \rangle = 0 & \text{for } n_i^F \le 0 \\ \langle n_i^F \rangle = n_i^F & \text{for } n_i^F > 0 \end{cases} \tag{26}$$

## 3.2 Derivation of the DSC incremental stress equation

Assuming the thickness of joint is the same for all three material phases, equilibrium of forces in the disturbed material, and the definition of disturbance in Eq. (17), the following relationship between phase stresses can be derived

$$\begin{Bmatrix} \sigma_n^a \\ \tau^a \end{Bmatrix} = \begin{Bmatrix} (1-D_n)\sigma_n^i \\ (1-D_\tau)\tau^i \end{Bmatrix} + \begin{Bmatrix} D_n \sigma_n^c \\ D_\tau \tau^c \end{Bmatrix} \tag{27}$$

where the normal disturbance function, $D_n$, can be used to model the relative normal displacements and $D_\tau$, is the disturbance function for relative shear displacements.

Differentiating Eq. (27),

$$\begin{Bmatrix} d\sigma_n^a \\ d\tau^a \end{Bmatrix} = \begin{Bmatrix} (1-D_n)d\sigma_n^i \\ (1-D_\tau)d\tau^i \end{Bmatrix} + \begin{Bmatrix} D_n d\sigma_n^c \\ D_\tau d\tau^c \end{Bmatrix} + \begin{Bmatrix} (\sigma_n^c - \sigma_n^i)dD_n \\ (\tau^c - \tau^i)dD_\tau \end{Bmatrix} \tag{28}$$

If there is no change in stresses at FA state, $d\sigma_n^c$ and $d\tau^c$ are zero. Substituting Eqs. (15) and (23) into Eq. (28) gives the DSC incremental stress-strain equations,

$$\begin{Bmatrix} d\sigma_n \\ d\tau^a \end{Bmatrix} = \begin{Bmatrix} (1-D_n)(C_{nn}^{ep} d\varepsilon_n^i + C_{ns}^{ep} d\gamma) \\ (1-D_\tau)(C_{sn}^{ep} d\varepsilon_n^i + C_{ss}^{ep} d\gamma) \end{Bmatrix} + \begin{Bmatrix} (\sigma_n^c - \sigma_n^i)dD_n \\ (\tau^c - \tau^i)dD_\tau \end{Bmatrix} \tag{29}$$

and

$$\{d\sigma^a\} = [C^{DSC}]\{d\varepsilon\} + \{dD(\sigma^c - \sigma^i)\} \tag{30}$$

where the term $\{dD(\sigma^c - \sigma^i)\}$ contributes negative values during softening and [CDSC] is DSC constitutive matrix.

## 4. Model parameters

The proposed joint model involves a number of material constants which can be determined from a series of shear tests on joints or interfaces. The material constants can be divided into three categories: parameters for RI material, the constants for FA material, and the disturbance function parameters. The material constants are all listed in Table 1. There are eleven parameters needed for the DSC joint model.

## 5. Verification of DSC model for rock joints

The disturbed state joint model derived and modified in previous section is verified with respect to comprehensive laboratory tests performed by Schneider (1974). For verification, the model back predictions are obtained by numerical integration formulation based on Equation(30).

Schneider (1974) performed a series of well designed shear tests. The samples of the joints are replicas made of plaster casts from a same natural rock joints. In doing so, many similar joints samples were produced and the influence of the normal stresses on the joint behavior was studied. For this research, the granite joint is utilized and investigated. The granite joint is relatively rough and has a high degree of indentation both on the microscopic as well as on the macroscopic scale.

For the granite joint, four tests were performed under different constant normal stresses. The normal stresses are 1.77MPa, 1.38MPa, 0.69MPa, and 0.34MPa, respectively. The back predictions of the four tests are shown from Fig.6 to Fig.10 and model parameters used in the back predictions are listed in Table 2. Fig. 6 shows the back prediction of the shear responses for the four tests under the four different normal stresses. the normal stress $\sigma_n$ is kept constant during each test and severe softening occurs for all four tests. Fig. 7 to Fig. 10 show the

Table 1. DSC joint parameters.

| Category | Parameter | Comments |
|---|---|---|
| RI Material | E | Young's Modulus |
| | υ | Poisson's Ratio |
| | n | Phase Change Parameter |
| | ɣ | Ultimate Parameter |
| | a | Hardening Parameter |
| | b | $\alpha = \frac{a}{\xi_D^b}$ |
| FA Material | $C^0$ | Critical Parameter |
| | $v^0$ | |
| | κ | |
| DSC Function | $A_n$, $Z_n$ | $D_n = [1 - \exp(-A_n \xi_D^{Z_n})]$ |
| | $A_\tau$, $Z_\tau$ | $D_n = [1 - \exp(-A_\tau \xi_D^{Z_\tau})]$ |

back predictions of the dilative responses.

In Fig. 6, it is shown that the back predictions have predicted softening behavior of the granite joint. The back predictions are very satisfactory for the two shear tests with low value of normal stresses (0.69MPa and 0.34MPa). Reasonably good predictions are shown for the two shear tests with higher normal stresses (1.77MPa and 1.38 MPa), but the high peaks of the shear stresses are not predicted by the back predictions. This is because the material parameters are found through an average process and the number of data points for the high peaks are too few to input a significant influence.

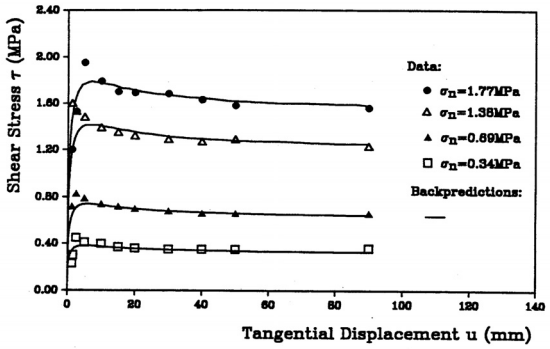


Fig. 6 Shear response for granite joint.

The difference of the normal stresses used in the

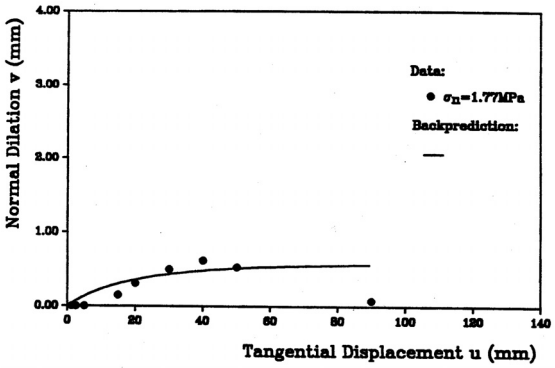


Fig. 7 Dilative response for granite joint with $\sigma_n$ =1.77MPa.

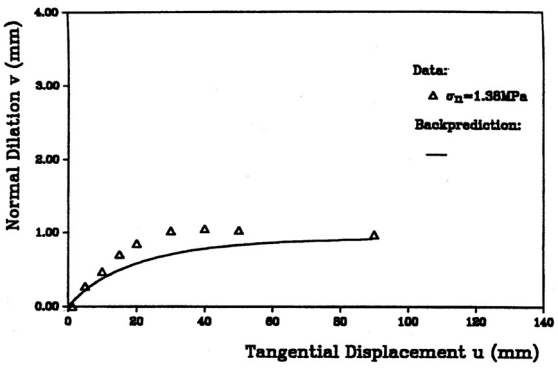


Fig. 8 Dilative response for granite joint with $\sigma_n$ =1.38MPa.

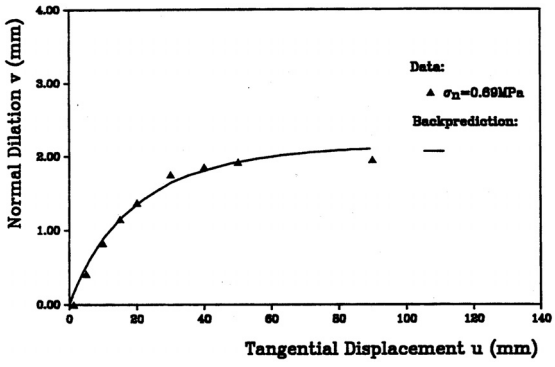


Fig. 9 Dilative response for granite joint with $\sigma_n$ =0.69MPa.

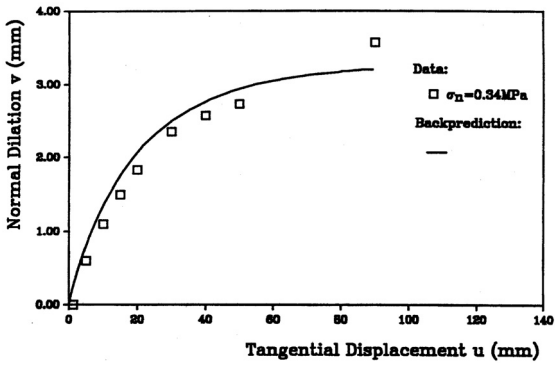


Fig. 10 Dilative response for granite joint with $\sigma_n$ =0.34MPa.

Table 2. Model parameters for back predictions.

| Category | Parameter | Values |
|---|---|---|
| RI Material | E | $E_n$=5.6MPa, $E_s$=28.0MPa |
| | υ | 0.30 |
| | n | 2.31 |
| | γ | 3.24 |
| | a | 0.065 |
| | b | 1.42 |
| FA Material | $C^0$ | 0.90 |
| | $v^0$ | 4.96 |
| | κ | 1.21 |
| DSC Function | $A_n$, $Z_n$ | $A_n$= 3.87, $Z_n$=0.36 |
| | $A_\tau$, $Z_\tau$ | $A_\tau$=3.88, $Z_\tau$=0.90 |

tests are large enough to cause a significant change in the dilative behavior for different normal stresses from Fig. 7 to Fig. 10. The back predictions for the dilative behavior are very good except for the test with normal stress $\sigma_n$ =1.77MPa, where large discrepancy can be observed in Fig. 7. This large discrepancy is due to the non-regularity of the data obtained from the test, possibly due to a catastrophic damage occurred to the asperities under such a high normal stress and consequently, the dilation reduces to a very small value at large stage of the shear process.

## 6. Conclusions

The disturbed state modeling provides a powerful way of describing the behavior of joints of tunnel. It is based on the assumption that the behavior of a joint, or the behavior at the disturbed state can be expressed by the joint behavior at its reference states.

The reference states include the original (RI) state and critical (FA) state. Basic models can be used to describe the simple behavior at the reference state and the complex behavior at the disturbed state can be described by using the disturbed state joint model.

From this study, the behavior of intact joint is modeled by using a general plasticity model with minor modifications. The FA state is modeled according to the observations from the shear tests of joints. The DSC joint model based on two reference states thus developed is capable of describing the hardening and softening behavior of a joint under various stress paths.

The model can be easily implemented in numerical integrated formulation procedures and requires a realistic number of parameters for general use. Finally, this model is capable of capturing essential rock joint behavior including strain softening using back prediction scheme.

## References


1. Archard, J.F. (1958), "Elastic Deformation and the Laws of Friction," Proc. Roy. Soc. London, A243, pp. 190-205.
2. Armaleh S.H. and Desai, C. S. (1990), "Modeling

Include Testing of Cohesionless Soils Under Disturbed State Concept," Report to the NSF, Dept. of Civil Engrg. and Engrg. Mech., Univ. of Arizona, Tucson.
3. Barton, N. R. and Chouby, V. (1977), "The Shear Strength of Rock Joints in Theory and Practice," *Rock Mechanics*, Vol.10, pp.1–54.
4. Desai, C. S., (1995), "Chapter 8: Constitutive modeling using the disturbed state as microstructure self–adjustment concept," *Continuum Models for Material with Microstructure*, H. B. Muhlhaus, ed., John Wiley & Sons, U. K.
5. Desai, C. S., (1992), "The disturbed state as transition through self–adjustment concept for modeling mechanical response of materials and interfaces," *Report*, Department of Civil Engineering and Engineering Mechanics, University of Arizona, Tucson, Arizona.
6. Desai, C. S. and Fishman, K. L. (1987), "Constitutive Models for Rocks and discontinuities (Joints)," Rock Mechanics: *Proc. 28th US Symp.*, (Farmer, L. W. et al., Ed.), University of Arizona at Tucson, pp.73–80.
7. Desai, C. S. and Fraque, M. O. (1984), "Constitutive Model for Geologic Materials," *J. of Eng. Mech. Div., ASCE*, Vol.110, No.9, pp.1391–1408.
8. Desai, C. S., Somasundaram, S., and Frantziskonis, G. (1986), "A Hierarchical Approach for Constitutive Modeling of Geologic Materials," *Int. J. for Num. and Analyt. Mech. in Geomech.*, Vol.10, No.3, pp.225–257.
9. Desai, C. S. and Wathugala, G. W. (1987), "Hierarchical and unified models for solids and discontinuities (Joints/Interfaces)," *Short Course Notes*, Workshop on Implementation of Constitutive Laws of Engineering Materials, Department of Civil Engineering and Engineering Mechanics, University of Arizona, Tucson, Arizona, pp.9–10, 31–124.
10. DiMaggio, F. L. and Sandler, I. S. (1971), "Material Model for Granular Soils," *J. of Eng. Mech. Div., ASCE*, Vol.97, No.EM3, pp.935–950.
11. Ghaboussi, J. and Wilson, E. L. (1973), "Finite Element for Rock Joints and Interfaces," *J. of Soil Mech. and Found. Div., ASCE*, Vol.99, No. SM10, pp.833–848.
12. Goodman, R. E. (1974), "The Mechanical Properties of Joints," *Proc., 3rd Cong. Int. Soc. of Rock Mech.*, Denver, Co, Vol.1, Part A, pp.127–140.
13. Goodman, R. E., Taylor, R. L., and Brekke, T. L. (1971), "A Model for the Mechanics of Jointed Rock," *J. of Soil Mech. and Found. Div., ASCE*, Vol.94, No.SM3, pp.637–659.
14. Hoek, E. and Bray, J. (1974), "Rock Slope Engineering," *J. of Min. and Metallurgy*, London.
15. Park, I. J., (1997), "Disturbed state modeling for dynamic and liquefaction analysis," *Ph.D. Dissertation*, Department of Civil Engineering and Engineering Mechanics, University of Arizona, Tucson, Arizona.
16. Plesha, M. E. (1987), "Constitutive Models for Rock Discontinuities with Dilatancy and Surface Degradation," *Int. J. for Num. and Analyt. Mech. in Geomech.*, Vol.11, pp.345–362.
17. Schneider, H. J. (1975), "Rock Friction–A Laboratory Investigation," *Proc. 3rd Cong. Int. Soc. Rock Mech.*, Denver, Co, Vol.2, Part A, pp.311–315.
18. Zienkiwicz, O. C. and Pande, G. N. (1977), "Time Dependent Multilaminate Model of Rocks – A Numerical Study of Deformation and Failure of Rock Masses," *Int. J. for Num. and Analyt. Mech. in Geomech.*, Vol.1, pp.219–247.

**박인준**

**한서대학교, 교수**

**geotech@hanseo.ac.kr**